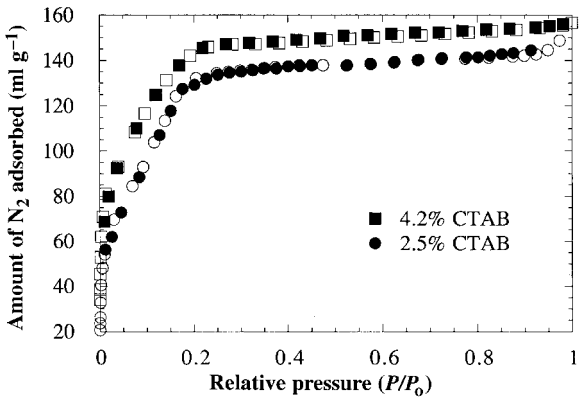

Figure 5 N_2 sorption isotherms obtained at 77 K for a 400-nm thick incipient 1-dH film prepared with $c_o = 0.06$ M (adsorption, white circles; desorption, black circles) and a 250-nm-thick cubic 3-dH film prepared with $c_0 = 0.10$ M (adsorption, white squares; desorption, black squares). The films were applied to ~1 cm^2 area of a piezoelectric ST-cut quartz substrate with interdigital gold transducers designed to operate at ~97 MHz. Mass change was monitored (~80 pg cm^{-2} sensitivity) as a function of relative pressure using a surface acoustic wave technique[21].

membrane lipid/water systems[19]. It has been suggested that two lipid bilayers transform through an inverted micellar intermediate to a cubic mesophase[20]. We propose that the 3-dH film is derived from the parent cubic film by constrained one-dimensional shrinkage during calcination[3]. The cubic → 3-dH transformation can be considered as a constrained one-dimensional distortion of the cubic cell along the [110]-direction. Comparable lattice parameters between the two mesophases allow seamless transitions between ordered domains and cause cubic and 3-dH domains to be essentially indistinguishable in plan-view (Fig. 4c).

A surface acoustic wave technique[21] was used to determine pore accessibility of supported films. Figure 5 compares nitrogen sorption isotherms of the incipient 1-dH and cubic 3-dH films. Despite the substantially different degrees of ordering, the isotherms are qualitatively similar. The lack of hysteresis and absence of any appreciable adsorption at relative pressures above 0.3 is consistent with a unimodal porosity with no interparticle meso- or macroporosity[22]. The surface areas calculated for the cubic 3-dH and incipient 1-dH films are 734 and 648 $m^2 g^{-1}$, respectively, demonstrating the accessibility of the mesophase porosity. In addition, the trans-film flux of cubic 3-dH films prepared as supported membranes increased by over 1,000× upon calcination, establishing through-thickness pore connectivity (A. Tsai, unpublished results).

We have demonstrated a rapid, continuous process, enabling the practical utilization of mesostructures in thin-film form. The uniform three-dimensional pore channel systems of cubic 3-dH films and the absence of granularity suggest applications in molecular separation, catalysis and sensors. The dip-coating procedure combined with the optical probe technique enables us to follow the progressive evolution of the mesostructured films and should provide insight into the synthesis of complex, self-organized organic/inorganic assemblies in general[23]. □

Received 24 June; accepted 16 July 1997.

1. Kresge, C. T., Leonowicz, M. E., Roth, W. J., Vartuli, J. C. & Beck, J. S. Ordered mesoporous molecular sieves synthesized by a liquid-crystal template mechanism. *Nature* **359,** 710–712 (1992).
2. Beck, J. S. *et al.* A new family of mesoporous molecular sieves prepared with liquid crystal templates. *J. Am. Chem. Soc.* **114,** 10834–10843 (1992).
3. Yang, H., Kuperman, A., Coombs, N., Mamiche-Afara, S. & Ozin, G. A. Synthesis of oriented films of mesoporous silica on mica. *Nature* **379,** 703–705 (1996).
4. Yang, H., Coombs, N., Sokolov, I. & Ozin, G. A. Free-standing and oriented mesoporous silica films grown at the air–water interface. *Nature* **381,** 589–592 (1996).
5. Aksay, I. A. *et al.* Biomimetic pathways for assembling inorganic thin films. *Science* **273,** 892–898 (1996).
6. Ogawa, M. Formation of novel oriented transparent films of layered silica-surfactant nanocomposites. *J. Am. Chem. Soc.* **116,** 7941–7942 (1994).
7. Ogawa, M. A simple sol-gel route for the preparation of silica-surfactant mesostructured materials. *Chem. Commun.* 1149–1150 (1996).
8. Manne, S. & Gaub, H. E. Molecular organization of surfactants at solid–liquid interfaces. *Science* **270,** 1480–1482 (1995).
9. Brinker, C. J. *et al.* in *Access in Nanoporous Materials* (eds Pinnavaia, T. J. & Thorpe, M. F.) 123–139 (Plenum, New York, 1995).
10. Brinker, C. J. & Scherer, G. W. in *Sol–Gel Science* 120 (Academic, San Diego, 1990).
11. Brinker, C. J., Hurd, A. J., Schunk, P. R., Frye, G. C. & Ashley, C. S. Review of sol-gel thin film formation. *J. Non-Cryst. Solids* **147, 148,** 424–436 (1992).
12. Nishida, F. *et al. In situ* fluorescence probing of the chemical-changes during sol-gel thin-film formation. *J. Am. Ceram. Soc.* **78,** 1640–1648 (1995).
13. Shinitzky, M., Dianoux, A. C., Gitler, C. & Weber, G. Microviscosity and order in the hydrocarbon region of micelles and membranes determined with fluorescent probes: I, Synthetic micelles. *Biochemistry* **10,** 2106–2113 (1971).
14. Auvray, X., Petipas, C., Anthore, R., Rico, I. & Lattes, A. X-ray diffraction study of mesophases of cetyltrimethylammonium bromide in water, formamide, and glycerol. *J. Phys. Chem.* **93,** 7458–7464 (1989).
15. Ryoo, R., Kim, J. M., Ko, C. H. & Shin, C. H. Disordered molecular sieve with branched mesoporous channel network. *J. Phys. Chem.* **100,** 17718–17721 (1996).
16. Pashley, R. M. & Israelachvili, J. N. A comparison of surface forces and interfacial properties of mica in purified surfactant solutions. *Colloids Surf.* **2,** 169–187 (1981).
17. Monnier, A. *et al.* Cooperative formation of inorganic organic interfaces in the synthesis of silicate mesostructures. *Science* **261,** 1299–1303 (1993).
18. Israelachvili, J. N., Mitchell, D. J. & Ninham, B. W. Theory of self-assembly of hydrocarbon amphiphiles into micelles and bilayers. *J. Chem. Soc.* **2,** 1525–1568 (1976).
19. Lindblom, G. & Reifors, L. Cubic phases and isotropic structures formed by membrane lipid—possible biological relevance. *Biochim. Biophys. Acta* **988,** 221–256 (1989).
20. Siegel, D. Inverted micellar structures in bilayer membranes. *J. Biophys.* **45,** 399–420 (1986).
21. Frye, G. C., Ricco, A. J., Martin, S. J. & Brinker, C. J. Characterization of the surface area and porosity of sol-gel films using SAW devices. *Mat. Res. Soc. Symp. Proc.* **121,** 349–354 (1988).
22. Greg, S. J. & Sing, K. S. W. *Adsorption, Surface Area, and Porosity* 2nd edn (Academic, New York, 1982).
23. Mann, S. & Ozin, G. A. Synthesis of inorganic materials with complex form. *Nature* **382,** 313–318 (1996).

Acknowledgements. We thank S. Singh, A. Tsai, M. Rodriguez, M. Eatough and R. Tissot for assistance with experiments and M. Aragon for technical illustrations. This work was partially supported by the UNM/NSF Center for Micro-Engineered Materials, by grants from the NSF, by the DOE Basic Energy Sciences, the Electric Power Research Institute and the DOE Federal Energy Technology Center. This work was done under contract from the US Department of Energy. Sandia is a multiprogram laboratory operated by Sandia Corporation, a Lockheed Martin Company, for the US Department of Energy.

Correspondence and requests for materials should be addressed to C.J.B. (e-mail: cjbrink@sandia.gov).

Extraction of a hydrophilic compound from water into liquid CO_2 using dendritic surfactants

A. I. Cooper*, J. D. Londono†‡, G. Wignall†, J. B. McClain*, E. T. Samulski*, J. S. Lin†, A. Dobrynin*, M. Rubinstein*, A. L. C. Burke*, J. M. J. Fréchet§ & J. M. DeSimone*

* *Department of Chemistry, CB#3290, Venable and Kenan Laboratories, University of North Carolina at Chapel Hill, Chapel Hill, North Carolina 27599-3290, USA*
† *Oak Ridge National Laboratory, Oak Ridge, Tennessee 37381-6031, USA*
‡ *Department of Chemical Engineering, University of Tennessee, Knoxville, Tennessee 37996-220, USA*
§ *Department of Chemistry, University of California-Berkeley, Berkeley, California 94720, USA*

Dendrimers are well defined, highly branched polymers[1–5] that adopt a roughly spherical, globular shape in solution. Their cores are relatively loosely packed and can trap guest molecules[5–7], and by appropriate functionalization of the branch tips the macromolecules can act as unimolecular micelle-like entities[6]. Here we show that dendrimers with a fluorinated shell are soluble in liquid carbon dioxide and can transport CO_2-insoluble molecules into this solvent within their cores. Specifically, we demonstrate the extraction of a polar ionic dye, methyl orange, from water into CO_2 using these fluorinated dendrimers. This observation suggests possible uses of such macromolecules for the remediation of contaminated water, the extraction of pharmaceutical products from fermentation vessels, the selective encapsulation of drugs for targeted delivery[6,7] and the transport of reagents for chemical

reactions (such as polymerization[8–11]) in liquid and supercritical CO_2 solvents.

Although CO_2 is a good solvent for many small molecules, only two classes of polymers have shown significant solubility (>10%) in CO_2 under practicable conditions (<100 °C and <350 bar); amorphous (and low-melting) fluoropolymers[8,12] and polysiloxanes[8,13]. As a result, there has been considerable effort to design fluorinated and siloxane-based surfactants that can stabilize dispersions of otherwise insoluble polymeric materials in carbon dioxide[9,10,13,14]. Small-angle X-ray scattering (SAXS) and small-angle neutron scattering (SANS) studies have shown that partially fluorinated amphiphilic surfactants can aggregate into micelles in carbon dioxide solution, the precise number of polymer chains per micelle being influenced by the CO_2 density[15–17].

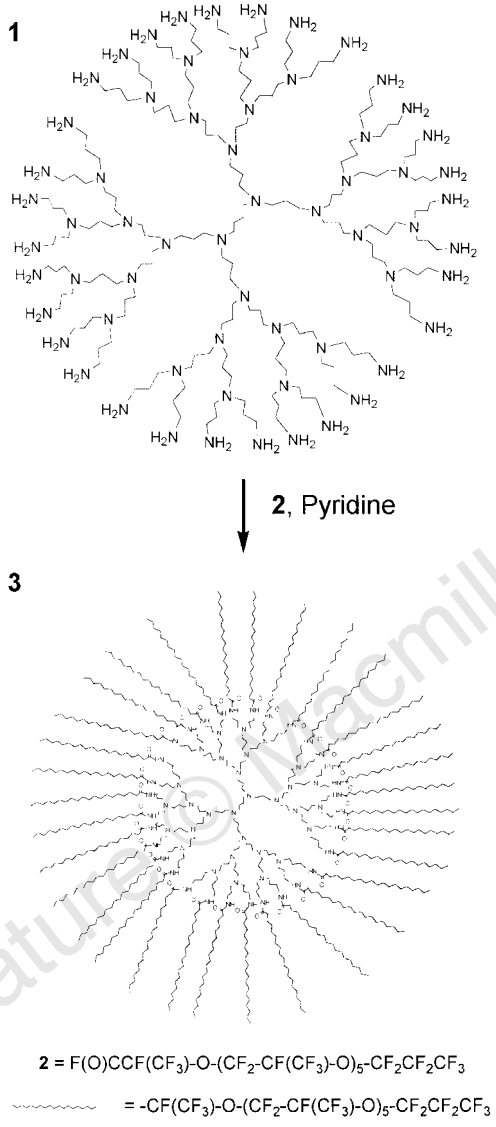

Figure 1 Synthesis of the unimolecular dendritic micelle. A solution of 2.92 g of **2** (35.2 equiv., 2.28 mmol) in freon 113 (50 ml) was added under argon to 0.25 g of DAB-*dendr*-$(NH_2)_{32}$ **1** (0.071 mmol) and 0.20 g pyridine (35.2 equiv., 2.28 mmol). The dendrimer **1** was insoluble in freon but was quite rapidly solubilized as the substitution reaction proceeded heterogeneously. Isolated yield after purification, 93%. ^{1}H NMR (freon 113/acetone-d_6): 8.70 (br, s, CON*H*-CH_2), 3.45 (br, s, CONH-CH_2), 2.40 (br, s, CH_2-N), 1.75 (br, s, $NCH_2CH_2CH_2N + NCH_2CH_2CH_2CH_2N$). ^{19}F NMR (freon 113/acetone-d_6): –76.72 to 79.81 (m, (O-CF(CF_3)CF_3)$_6$), –127.06, –127.48 ($CF_3CF_2CF_2O$), –129.21 (m, CF(CF_3)C(O)$NHCH_2$), ±142.32 (br, m, (O-CF(CF_3)CF_2)$_5$). Infrared (film): amide N–H stretch 3,350.7 cm^{-1}; C–H sat. 2,956.6, 2,835.9 cm^{-1}; amide C=O 1,709.5 cm^{-1}; N–H bend 1,540.9 cm^{-1}; C–F stretch 1,307.6, 1,235.2, 1,203.1, 1,146.8 cm^{-1}; C–O stretch 985.9 cm^{-1}. Ultraviolet–visible (freon 113): wavelengths 240, 273 nm. Differential scanning calorimetry: phase transitions at –58.5 °C and +27.6 °C. Elemental microanalysis: calculated for $C_{798}H_{403}F_{1181}N_{62}O_{202}$ (average 90% substitution) C, 26.01%; H, 1.11%; N, 2.38%; F, 61.63%; found C, 25.24%; H, 1.17%; N, 2.68%; F, 59.24%. Relative molecular mass (M_r): estimated from elemental analysis/^{1}H NMR (90% substitution), 36.4(±1.0) × 10^3; determined by small angle X-ray scattering, 33.5(±3.0) × 10^3.

The micelle-like structure investigated here is quite different. By extending methods developed by Meijer[6], a fourth-generation hydrophilic dendrimer[18], DAB-*dendr*-$(NH_2)_{32}$, **1**, was functionalized with a 'CO_2-philic' shell, derived from a heptamer acid fluoride of hexafluoropropylene oxide **2** $CF_3CF_2CF_2(OCF(CF_3)CF_2)_5$-$OCF(CF_3C(O)F$, thus generating what may be considered as a well-defined, CO_2-soluble, unimolecular dendritic micelle, **3** (compounds **1**, **2** and **3** are shown in Fig. 1). Characterization data agreed with a structure where, on average, 90% of the peripheral amine groups of **1** had been functionalized with perfluoropolyether chains. NMR spectroscopy showed that the N*H*CO proton signal for **3** (8.70 p.p.m.) was shifted significantly downfield from the corresponding signal at 7.75 p.p.m. for the single-chain model compound, $F_3CF_2CF_2O(CF(F_3)CF_2O)_5(CF(CF_3)C(O)N$*H*-$CH_2CH_2CH_3$, **4**. This is consistent with strong intramolecular hydrogen bonding between amide groups in the closely packed dendritic structure of **3**, as described previously for analogous systems[6]. We found the functionalized dendrimer **3** to be insoluble in water (<10 p.p.m.) and most common organic solvents (methanol, methylene chloride, tetrahydrofuran, hexanes, chloroform and acetone), but to be soluble at room temperature in liquid CO_2 at pressures above 76 atm (1,110 pounds per square inch). Dendrimer **1** was insoluble in CO_2 under the same conditions.

As many highly polar molecules are insoluble in carbon dioxide, we decided to investigate the potential of **3** as a host system for polar guests in CO_2. It has been demonstrated previously that guest molecules can be trapped in a permeable dendritic core *in situ* by constructing a dense shell around the impregnated core and generating a 'dendritic box'[19–21]. Alternatively, the dendritic core of a pre-formed, micelle-like host can be loaded with guest molecules in a homogeneous solution of both host and guest[6]. By contrast, we have concentrated on the micelle-assisted transfer of guest molecules between two immiscible phases. Quite surprisingly, we have

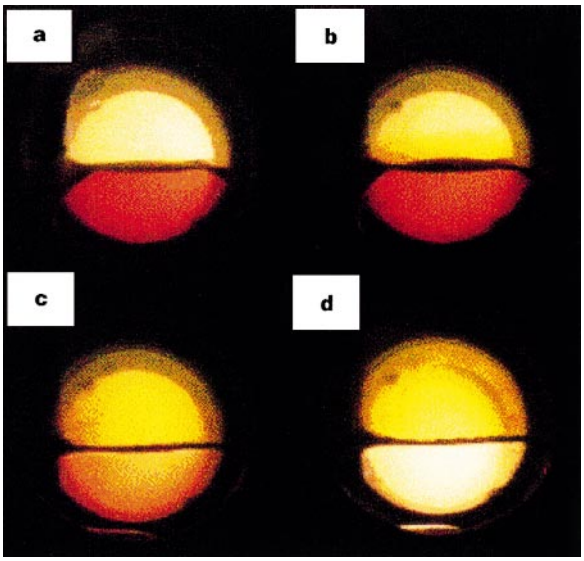

Figure 2 Diffusion of methyl orange (**5**) from aqueous solution (upper phase in figure) into a unimolecular dendritic micelle **3** in liquid CO_2 (lower phase) at 23.5 °C, 340 atm. Video images taken 1 min (**a**), 6 min (**b**), 30 min (**c**) and 150 min (**d**) after the addition of CO_2. Initial molar ratio of **5** : **3** = 1 : 60.

found that the dendritic micelle **3** can transfer methyl orange (**5**), a CO_2-insoluble ionic dye[22], from aqueous solution into carbon dioxide (Fig. 2). A small quantity of **3** was weighed onto one of the CaF_2 windows of a 2.5-ml high-pressure cell, the cell assembled, and an aqueous solution of **5** (3.30×10^{-3} mol l^{-1}) was added such that it did not come into contact with **3**. On addition of CO_2, the dendritic micelle dissolved rapidly, forming a colourless CO_2 phase (Fig. 2a). With time and in the absence of agitation, the colour in the aqueous phase decreased in intensity and a gradual colouring of the CO_2 layer was observed (Fig. 2b, c). After 150 min, it appeared that no dye remained in the aqueous phase (Fig. 2d). When the cell was depressurized, the dye-loaded micelle was deposited on the interior of the cell as a yellow film.

Spectroscopic analysis detected no dye in the residual aqueous phase, which suggests that under these conditions (a large excess of **3**) it was possible to extract this dye completely from the aqueous layer. No coloration of the CO_2 phase was observed in the absence of **3**. The wavelength of the ultraviolet absorption for **5** in the dendritic core of **3**/CO_2 (Fig. 3a) was found to be significantly shifted from the absorption of **5** in aqueous solution (425–430 nm compared to 464 nm), and also from the wavelength observed for **5** dissolved in a water-in-CO_2 microemulsions[23,24]. This wavelength shift is also evident from the difference in colour of the aqueous and CO_2 phases in Fig. 2. To calculate the maximum number of dye molecules that could occupy the dendritic core, experiments were conducted with varying molar ratios of **5** and **3** in the aqueous/CO_2 phases (Fig. 3b). In all cases, the growth of the ultraviolet absorption of **5** was monitored as a function of time until the absorbance reached a constant value, usually after 25–35 h at room temperature without stirring. The maximum integral absorbance was related to the concentration of the dye in the CO_2 phase, which was then used to calculate the number of dye molecules per micelle core. At low ratios of dye to micelle (for example, 1 : 1), it was possible to extract essentially all of the dye from the aqueous layer and, indeed, an average value of around one dye molecule per dendritic core was determined spectroscopically. This is important because it suggests that the extinction coefficient of the dye absorption does not change significantly in the dendrimer core, and also that our quantification methods are valid[6]. As the molar ratio of **5** to **3** was increased, the average dye loading increased accordingly, up to a maximum of around 12 dye molecules per dendritic core. Equivalent experiments were conducted with the dye rose bengal, **6** (Fig. 3b). The maximum number of dye molecules per dendritic core (around seven) was consistent with the somewhat larger size of this guest molecule (relative molecular mass, M_r, of **5**, 327.37; M_r of **6**, 1017.65), and was also comparable with Meijer's observations for alkyl modified dendrimers[6].

The precise mechanism by which the dyes migrate from the aqueous phase into the dendritic core in CO_2 is not yet known. As dyes **5** and **6** are essentially insoluble in the CO_2 phase and **3** is essentially insoluble in water, it seems conceivable that the highly plasticized dendritic micelle might adopt a distorted conformation at the water–CO_2 interface, such that the hydrophilic core comes in close proximity to the aqueous layer. Preliminary experiments using Reichardt's dye[25] as a solvatochromic probe for the effective polarity of the dendritic micelle interior[26] suggest that the diffusion of significant amounts of water into the micelle core may accompany the phase transfer of both **5** and **6**.

Small angle X-ray scattering measurements[16,27], using a high-pressure cell similar to that described previously[28], were used to estimate the radius of gyration and the relative molecular mass of the fluorinated dendrimer. Standard corrections were applied and the data were normalized to units of absolute differential scattering cross-section[29], $d\Sigma/d\Omega\ (Q)$ (cm^{-1}) where Σ denotes the total scattering cross-section, $d\Omega$ is the solid angle and Q is the scattering vector. Scattering data were collected at 340 atm and 25 °C for a number of concentrations of **3** in CO_2. Data were fitted to a variable arm number star model (an 'f-arm star model') over the whole range of Q, and linear fits were also obtained for $[d\Sigma/d\Omega\ (Q)]^{-1}$ versus Q^2, in the range $0.01 \leqslant Q \leqslant 0.05$ Å^{-1}. The radius of gyration, R_g derived from the f-arm star fits for **3** in CO_2 was 30.0 ± 1.0 Å. The value of R_g did not vary significantly with concentration, which suggests that no particle aggregation occurred in the CO_2 solution under these conditions. A plot of

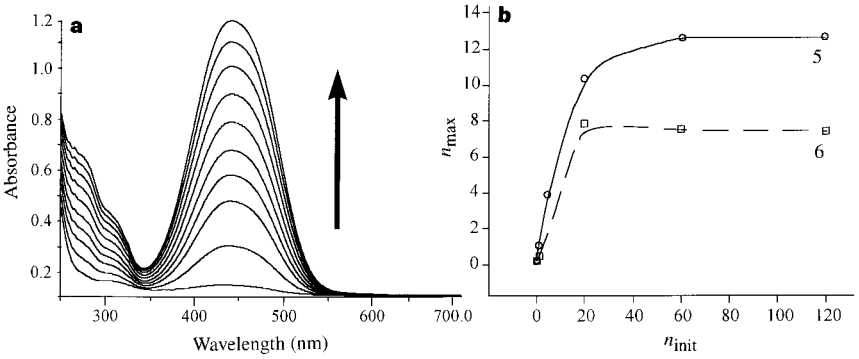

Figure 3 a, Ultraviolet–visible spectra illustrating the diffusion of methyl orange (**5**) from an aqueous phase into a unimolecular dendritic micelle **3** in liquid CO_2 (24.9 °C, 340 atm). Spectra taken every 30 min. The high-pressure cell was arranged so that the ultraviolet beam passed only through the CO_2 phase. Molar ratio of **5** : **3** = 60 : 1. **b**, Maximum number of guest molecules per micelle core (n_{max}) for methyl orange (trace labelled '5') and rose bengal (trace labelled '6') versus the initial molar ratio (n_{init}) of **5** : **6**.

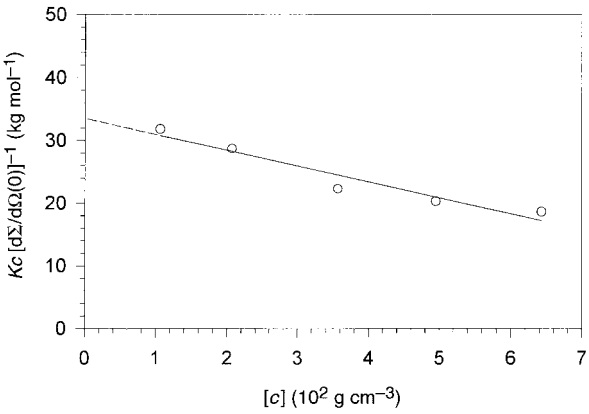

Figure 4 Plot of $K_d[d\Sigma/d\Omega(0)]^{-1}$ versus concentration (c) for the dendritic micelle **3** in liquid CO_2 (23.7C, 340 atm); see text. $K = (\rho_p - \rho_s)^2 A_0 V_p^2 c/[d\Sigma/d\Omega(0)]$, where ρ_p and ρ_s are the scattering length densities of particle and solvent, A_0 is Avogadro's number and V_p is the estimated particle volume.

$Kc[d\Sigma/d\Omega\,(0)]^{-1}$ versus concentration of **3** is shown in Fig. 4, based on the $d\Sigma/d\Omega\,(0)$ values derived from f-arm star fits. (Here K is the SAXS contrast factor and c is the concentration.) The intercept at zero concentration gives the weight average relative molecular mass for **3** to be $33.5(\pm 3.0) \times 10^3$ which is consistent with values obtained by ^{1}H NMR and elemental microanalysis ($36.4(\pm 1.0) \times 10^3$). The M_r value derived from linear (Zimm) fits was within 0.3% of the value derived from the f-arm star fits.

These experiments demonstrate that surfactant-modified CO_2 can be used to enhance dramatically the applicability of supercritical-fluid extraction applications using environmentally benign CO_2 to replace some of the billions of pounds of organic solvents used every year in extraction and cleaning applications. □

Received 4 April; accepted 7 July 1997.

1. Tomalia, D. A. *et al*. A new class of polymers: starburst-dendritic macromolecules. *Polym. J.* **17,** 117–132 (1985).
2. Hawker, C. J., Lee, R. & Frechet, J. M. J. One-step synthesis of hyperbranched dendritic polyesters. *J. Am. Chem. Soc.* **113,** 4583–4588 (1991).
3. Frechet, J. M. J. Functional polymers and dendrimers: reactivity, molecular architecture, and interfacial energy. *Science* **263,** 1710–1715 (1994).
4. Knapen, J. W. J. *et al*. Homogeneous catalysts based on silane dendrimers functionalized with arylnickel(II) complexes. *Nature* **372,** 659–663 (1994).
5. Newkome, G. R., Moorefield, C. N. & Voegtle, F. *Dendritic Molecules: Concepts, Syntheses, Perspectives* (VCH, Weinheim, 1996).
6. Stevelmans, S. *et al*. Synthesis, characterization and guest-host properties of inverted unimolecular dendritic micelles. *J. Am. Chem. Soc.* **118,** 7398–7399 (1996).
7. Hawker, C. J., Wooley, K. L. & Frechet, J. M. J. Unimolecular micelles and globular amphiphiles: dendritic macromolecules as novel recyclable solubilization agents. *J. Chem. Soc. Perkin I* 1287–1297 (1993).
8. DeSimone, J. M., Guan, Z. & Eisbernd, C. S. Synthesis of fluoropolymers in supercritical carbon dioxide. *Science* **257,** 945–947 (1992).
9. DeSimone, J. M. *et al*. Dispersion polymerizations in supercritical carbon dioxide. *Science* **265,** 356–359 (1994).
10. Hsiao, Y.-L., Maury, E. E., DeSimone, J. M., Mawson, S. & Johnston, K. P. Dispersion polymerization of methyl methacrylate stabilized with poly(1,1-dihydroperfluorooctylacrylate) in supercritical carbon dioxide. *Macromolecules* **28,** 8159–8166 (1995).
11. Cooper, A. I. & DeSimone, J. M. Polymer synthesis and characterization in liquid/supercritical carbon dioxide. *Curr. Opin. Solid State Mater. Sci.* **1,** 761–768 (1996).
12. McHugh, M. A. & Krukonis, V. J. *Supercritical Fluid Extraction* 2nd edn (Butterworth-Heinman, Stoneham, MA, 1994).
13. Shaffer, K. A., Jones, T. A., Canelas, D. A. & DeSimone, J. M. Dispersion polymerizations in carbon dioxide using siloxane-based stabilizers. *Macromolecules* **29,** 2704–2706 (1996).
14. Canelas, D. A., Betts, D. E. & DeSimone, J. M. Dispersion polymerization of styrene in supercritical carbon dioxide: importance of effective sufactants. *Macromolecules* **29,** 2818–2821 (1996).
15. McClain, J. B. *et al*. Design of nonionic surfactants for supercritical carbon dioxide. *Science* **274,** 2049–2052 (1996).
16. Fulton, J. L. *et al*. Aggregation of amphiphilic molecules in supercritical carbon dioxide: a small angle X-ray scattering study. *Langmuir* **11,** 4241–4249 (1995).
17. McClain, J. B. *et al*. Solution properties of a CO_2-soluble fluoropolymer via small angle neutron scattering. *J. Am. Chem. Soc.* **118,** 917–918 (1996).
18. de Brabander-van den Berg, E. M. M. & Meijer, E. W. Poly(propylene imine) dendrimers: large-scale synthesis by heterogeneously catalyzed hydrogenations. *Angew. Chem. Int. Edn Eng.* **32,** 1308–1311 (1993).
19. Jansen, J. F. G. A., de Brabander-van den Berg, E. E. M. & Meijer, E. W. Encapsulation of guest molecules into a dendritic box. *Science* **266,** 1226–1229 (1994).
20. Bosman, A. W., Jansen, J. F. G. A., Janssen, R. A. J. & Meijer, E. W. Charge transfer in the dendritic box. *Polym. Mater. Sci. Eng.* **73,** 340–341 (1995).
21. Jansen, J. F. G. A., Meijer, E. W. & de Brabander-van den Berg, E. M. M. The dendritic box: shape-selective liberation of encapsulated guests. *J. Am. Chem. Soc.* **117,** 4417–4418 (1995).
22. Maury, E. E. *et al*. Graft copolymer surfactants for supercritical carbon dioxide applications. *Polym. Prepr. (ACS Div. Polym. Chem.)* **34,** 664–665 (1993).
23. McFann, G. J., Johnston, K. P. & Howdle, S. M. Solubilization in nonionic reverse micelles in carbon dioxide. *Am. Inst. Chem. Eng. J.* **40,** 543–555 (1994).
24. Johnston, K. P. *et al*. Water-in carbon dioxide microemulsions: an environment for hydrophiles including proteins. *Science* **271,** 624–626 (1996).
25. Reichhardt, C. Empirical parameters of solvent polarity as linear free-energy relationships. *Angew. Chem. Int. Edn Engl.* **18,** 98–110 (1979).
26. Zacharlasee, K. A., Phuc, N. V. & Kozanklewicz, B. Investigation of micelles, microemulsions, and phospolipid bilayers with the pyridinium n-phenolbetaine $E_t(30)$, a polarity probe for aqueous interfaces. *J. Phys. Chem.* **85,** 2676–2683 (1981).
27. Wignall, G. D. *et al*. Reduction of parasitic scattering in SAXS by a three-pinhole collimating system *J. Appl. Crystallogr.* **23,** 241–246 (1990).
28. Pfund, D. M., Zemanian, T. S., Linehan, J. C., Fulton, J. L. & Yonker, C. R. Fluid structure in supercritical xenon by nuclear magnetic resonance spectroscopy and small angle X-ray scattering. *J. Phys. Chem.* **98,** 11846–11857 (1994).
29. Russell, T. P., Lin, J. S., Spooner, S. & Wignall, G. D. Intercalibration of small angle X-ray and neutron scattering data. *J. Appl. Crystallogr.* **21,** 629–638 (1988).

Acknowledgements. A.I.C. thanks the Royal Commission for The Exhibition of 1851 for a research fellowship (1995–96); J.D.L. thanks the NSF for support through the University of Tennessee. We also acknowledge support from the NSF for a Presidential Faculty Fellowship (J.M.D., 1993–97) as well as from the Consortium on Synthesis and Processing of Polymeric Materials in CO_2, which is sponsored by the NSF, the Environmental Protection Agency, DuPont, Hoechst-Celanese, Air Products and Chemicals, B. F. Groodrich, Eastman Chemical, Bayer and Xerox. We also thank the Division of Material Sciences, US Department of Energy under contract with Lockheed-Martin Research Corporation, and the Exxon Education Fundation for support.

Correspondence and requests for materials should be addressed to J.M.D. (e-mail: desimone@unc.edu).

An Earth-like numerical dynamo model

Weijia Kuang & Jeremy Bloxham

Department of Earth and Planetary Sciences, Harvard University, 20 Oxford Street, Cambridge, Massachusetts 02138, USA

The mechanism by which the Earth and other planets maintain their magnetic fields against ohmic decay is among the longest standing problems in planetary science. Although it is widely acknowledged that these fields are maintained by dynamo action, the mechanism by which the dynamo operates is in large part not understood. Numerical simulations of the dynamo process in the Earth's core[1–4] have produced magnetic fields that resemble the Earth's field, but it is unclear whether these models accurately represent the extremely low values of viscosity believed to be appropriate to the core. Here we describe the results of a numerical investigation of the dynamo process that adopts an alternative approach[5] to this problem in which, through the judicious choice of boundary conditions, the effects of viscosity are rendered unimportant. We thereby obtain a solution that at leading order operates in an Earth-like dynamical regime. The morphology and evolution of the magnetic field and the fluid flow at the core–mantle boundary are similar to those of the Earth, and the field within the core is qualitatively similar to that proposed on theoretical grounds[6].

The dynamical regime of the geodynamo is most simply understood by considering the momentum balance in the Earth's fluid outer core. In addition to pressure gradients which play an essentially passive role, the leading order force balance is between the Coriolis force, the Lorentz force and the buoyancy force. Taylor[7] showed that the magnetic field must then adjust so that the axial Lorentz torque on the surface of any cylinder in the core coaxial with the rotation axis (the so-called Taylor torque) is small, because the only torques available to balance it arise from the viscous force and from inertia, both of which are small. In the so-called magnetostrophic limit, the effects of inertia and viscosity vanish, and the Taylor torques must then be zero; in this limit the dynamo is described as being in a Taylor state.

In the Earth, small deviations from the Taylor state result in torsional oscillations in which the Taylor torque is balanced to leading order by inertia, with viscous effects most probably playing only a very small role. This regime is not easily modelled numerically, because the extremely small values of the viscosity that are required to reach such a quasi-Taylor-state result in viscous boundary layers far thinner than those that can be resolved numerically. In the Earth, the viscous boundary layer thickness lies in the range from 3 cm to 100 m, depending on whether the primary mechanism of viscous dissipation is molecular or turbulent, which is very small compared to the radius of the core of almost 3,500 km.

This view of the force balance in the geodynamo is supported by observations that suggest that changes in the angular momentum of the core are well described by torsional oscillations about a Taylor state[8–10]. An alternative[11] is that the residual Taylor torques are balanced by viscous stresses at the boundaries. However, that model implies that angular momentum transfer between the outer core and mantle occurs on a timescale much longer than that suggested by observations.

Glatzmaier and Roberts[1–4] have developed a numerical dynamo model which produces a predominantly dipolar field, similar to the Earth's field, and a westward drift of the field, at a rate similar to the Earth's field. However, it is unclear whether viscous effects are sufficiently small in their model, for not only is the value that they